

# Chapter 23

## Molecular Insights About Gas Hydrate Formation



Omkar Singh Kushwaha, Sheshan B. Meshram, G. Bhattacharjee and Rajnish Kumar

**Abstract** At present, gas hydrates are the most abundant source of methane on the earth and could be a promising option in the context of climate change and energy challenges in the upcoming years. It is estimated that nearly 20,000 trillion cubic meters of methane gas is trapped in the naturally existing gas hydrate reserves. This amount will be sufficient to fulfill the energy requirements for centuries, even if 20–30% of methane is recovered by using recently developed technologies. Although gas hydrates have immense energy potential on the one hand, gas hydrate plugging, on the other hand, is one of the major industrial challenges that can cause huge economic losses. The increasing energy demand has led to drilling of deeper oil wells and has increased the length of transmission lines. The problems associated with hydrate formation have gained more attention from both researchers and industries. The current methods of combating gas hydrate plugging involve the use of methanol and ethylene glycol in a large concentration, which usually shifts the three-phase boundary region from hydrate stability region and prevents hydrate plugging. However, a large portion of these chemicals ends up in the gas stream. In such scenarios, the use of kinetic hydrate inhibitors (KHIs) becomes attractive, since these additives are required in low concentrations. The KHIs delay the nucleation of hydrate or decrease the kinetics of gas hydrate formation or both can occur simultaneously. In this work, we have reported the effect of three low molecular weight di-acids, namely oxalic acid, malonic acid and succinic acid on synthetic natural gas hydrate formation kinetics. The di-acids were tested at two molar concentrations of 0.01 and 0.05 M at 3.0 MPa and 273.15 K. The hydrate former gas consumption and induction time data are reported, and discussion on the nature of results is also presented in this work.

---

O. S. Kushwaha (✉) · S. B. Meshram · G. Bhattacharjee · R. Kumar  
Chemical Engineering Department, Indian Institute of Technology-Madras, Chennai 600036,  
Tamil Nadu, India  
e-mail: [kushwaha.iitmadr@gmail.com](mailto:kushwaha.iitmadr@gmail.com)

© Springer Nature Singapore Pte Ltd. 2019  
D. K. Singh et al. (eds.), *Advances in Spectroscopy: Molecules to Materials*,  
Springer Proceedings in Physics 236, [https://doi.org/10.1007/978-981-15-0202-6\\_23](https://doi.org/10.1007/978-981-15-0202-6_23)

311

## 23.1 Introduction

Gas hydrates or clathrate hydrates (inclusion compounds) are known to be nonstoichiometric crystalline water-based solids, physically resembling ice, in which the gas (guest) molecules are trapped inside the three-dimensional cages of hydrogen-bonded frozen water (host) molecules [1, 2]. One of the major differences between hydrate and ice is that ice forms as a pure component, whereas hydrate will not form without guest molecules of proper size which are generally gas molecules. Methane ( $\text{CH}_4$ ), ethane ( $\text{C}_2\text{H}_6$ ), propane ( $\text{C}_3\text{H}_8$ ) and carbon dioxide ( $\text{CO}_2$ ) are some common gases which form gas hydrates. Most of the naturally occurring hydrates are formed from  $\text{CH}_4$ . These are considered as a vast source of energy [1]. One volume of methane gas hydrate can significantly store nearly 160 volumes of methane gas [2]. Moreover, gas hydrates also have a significant role to play in (a) seawater desalination, (b) easy storage and transportation of gas and (c) carbon dioxide capture through hydrate formation and decomposition cycle [3]. Hydrates are generally stable at high pressure and low temperature conditions. Since gas hydrates usually consist of more than 85 mol% water, their properties are considered to be in variations of those of ice. For example, the mechanical strength of gas hydrates is nearly 20 times more than that of ice [4]. A unique property of clathrates is the absence of chemical bonding (between host and guest molecules), which makes it possible to separate them easily. When these hydrates are brought into normal temperature and pressure conditions they dissociate and convert back into water and gas. Gas hydrates are mostly present in two structures, namely cubic structure I (sI) and cubic structure II (sII) [5], whose structural details are highlighted in Fig. 23.1 [6]. However, it is also discovered that hydrates can exist in structure H (sH) form which is less likely to be found naturally [7].

Temperature and pressure in transmission lines can cross the equilibrium temperature and pressure leading to hydrate formation, thus plugging the pipelines. A plug formed in pipeline results in two zones, namely high-pressure zone between well or gas-rich zone and the plug, and a low-pressure zone is developed above the plug or other side of high-pressure zone. This may lead to very dangerous situation wherein the plug is likely to become a projectile upon high pressure difference between two zones [8]. Plugging in the transmission line often leads to intermittent stoppages in production, hence hampering the economics of the industries. Thus, inhibition of gas hydrate formation becomes important.

Hydrate prevention can be achieved by four methods: (a) hydraulic method (depressurization process), (b) mechanical method (pipeline pigging), (c) thermal process and (d) chemical addition [9]. Depressurization of pipelines on both sides results in quick conversion of hydrate plug into ice plug, which in turn takes longer time to melt as compared to gas hydrate [10]. However, depressurization is not suitable for pipelines carrying liquid hydrocarbons because reduction in pressure can lead to vaporization. In pipeline pigging, pipeline pigs are used as projectile to clear any obstacles or plug in their path. Thermal method requires heat input in plug region in pipeline to melt the hydrate by pushing the temperature above hydrate formation

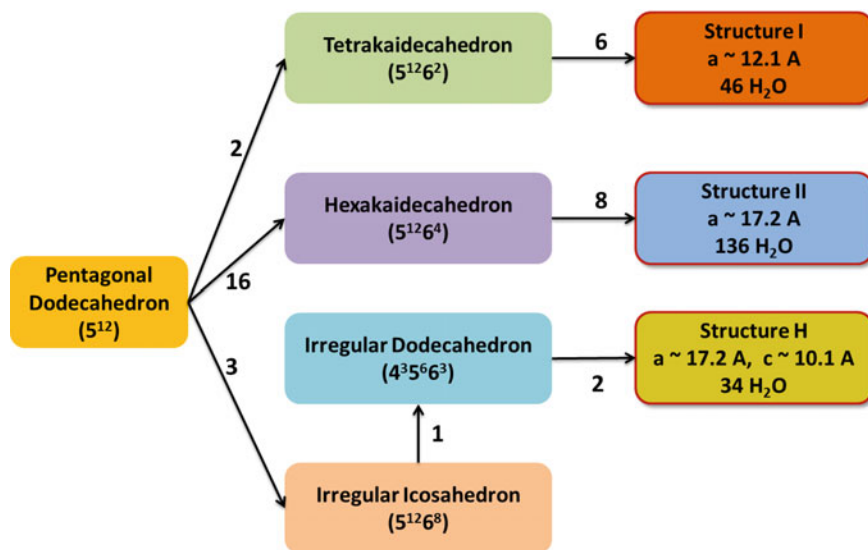


**Fig. 23.1** Different structures of gas hydrate cages. The numerical values indicated over arrows after each polyhedral cage structure indicates their final number in the unit cell of the particular gas hydrate structure type. The superscripted numbers indicate the number of respective membered closed-ring polyhedral structures formed by the host molecules (mostly water). The cells dimensions are also mentioned in angstrom units [6]

temperature. However, this method is applied for external application and not suitable for subsea conditions [9]. The three major chemical methods based on the action of additives are: thermodynamic inhibition, kinetic inhibition and anti-agglomeration.

The thermodynamic inhibitors' (THIs) action is totally different because they affect the chemical potential, and thus change the equilibrium dissociation curve to a less favorable region (tough to form hydrates). Additionally, thermodynamic inhibitors are usually required in higher concentrations ranging from 10 to 60 wt%, thus are costly means of inhibition. The most preferred thermodynamic inhibitors are methanol, ethanol and ethylene glycols. Further, the requirement of large storage and injection units, high recovery costs from wastewater and environmental hazards due to hydrocarbon fraction is unavoidable to search for new class of inhibitors [11, 12].

The kinetic inhibitors (KHIs), as an additive, are known to reduce the kinetics of hydrate formation either by delaying the nucleation of gas hydrates or by reducing the rate of growth of hydrate, or sometimes both can occur concomitantly. As a result, KHIs allow the transport of fluids from end to end without effective plugging of pipeline with gas hydrates (till hydrate formation takes place or delayed). In comparison to high volumes of THIs, the KHIs are required at significantly lower concentrations ranging from 0.1 to 1 wt% of active components. At present,

poly(vinylpyrrolidone) (PVP) and poly(vinylcaprolactam) (PVCap) are most commonly used KHIs for industrial as well as research purposes [5]. Chemically, KHIs are known to be water-soluble or have high water dispersibility [12].

Anti-agglomerants (AAs) act as dispersants which are new as compared to THIs and KHIs, and are required in lower concentrations >1 wt%. Their functioning is simple since they avoid the agglomeration of the hydrate crystals which further prevents the plugging of fluid transmission pipeline. Because of lesser agglomeration of gas hydrate crystals, AAs result in mobile slurry of gas hydrates [5]. The most commonly known new-generation AA is quaternary ammonium bromide (QAB) [13]. Owing to their low required concentrations, KHIs and AAs are known as low-dosage hydrate inhibitors (LDHI) and are currently of greater interest than THIs [5].

When a hydrophobic gas molecule enters water, water molecules arrange themselves forming a cage-like structure to encapsulate the gas molecule inside. It is found that the presence of hydrophobic moieties in the water can be helpful in stabilizing the nonpolar methane molecules [14]. The present study aims to study the effect of variation of alkyl chain length (hydrophobic moiety) on inhibition of gas hydrates. To solubilize additives, the presence of polar functional groups becomes vital; therefore the molecules having carboxyl groups were deliberately administered in this study. The experiments were performed at two concentrations (0.01 and 0.05 M) to study deviation in the promotion or inhibition activity due to change in concentrations (in the order of five times). All the experiments were carried out at identical conditions (3.0 MPa and 273.15 K) enabling the comparison of the properties.

## 23.2 Experimental Details and Procedure

### 23.2.1 Materials

High purity chemicals (purity 99%) were obtained from SRL Pvt. Ltd., India. All the chemicals were used without any additional treatment. Synthetic natural gas (SNG) was obtained from Indo Gas Agency, India. Detailed composition of natural gas is mentioned in Table 23.1.

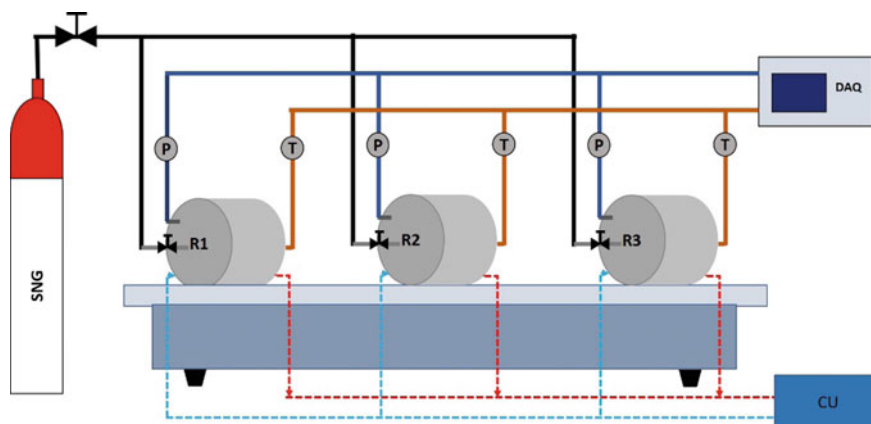
**Table 23.1** Composition of synthetic natural gas (SNG)

S. N.	Natural gas composition	Mole %
1.	Carbon dioxide	1.91
2.	Methane	88.4
3.	Ethane	5.80
4.	Propane	3.45
5.	N-butane + iso-butane	1.50

### 23.2.2 Experimental Setup and Reactor Design

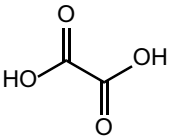
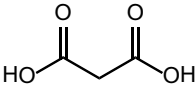
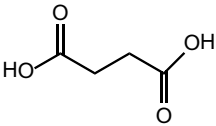
A newly fabricated shaking bed reactor (SBR) was used for the experimental hydrate inhibition studies. It consisted of three stainless-steel batch reactors fixed horizontally on a shaking bed using metal clamps. All the reactors were provided with pressure transducer (Wika, range 0–16 MPa) and thermocouple (RTD-Pt) with an accuracy of  $\pm 0.1$  K. Low temperature was maintained from the attached cooling unit to provide the desired temperatures inside the reactors. A stainless-steel ball (*diameter 20.8 mm*) was used in each of the reactors to disturb the gas–liquid interface and to create turbulence upon shaking. A data acquisition system (*PPI-make*) was used to collect the temperature and pressure data periodically. All reactors were insulated properly to reduce the heat transfer (heat-loss) from surroundings. The experimental setup and reactor design details are shown in Fig. 23.2.

After attaining the required temperature, the reactors were subjected to flushing by quick pressurization and depressurization cycles of SNG. All the three reactors were pressurized together to a predetermined experimental pressure of 3.0 MPa with SNG which is greater than its equilibrium pressure of 0.685 MPa at 273.15 K, thus providing sufficient driving force for SNG hydrate formation. The shaking bed was set at 80 rpm, an optimum from the trail experiments with water. Temperature and pressure were recorded at every 5 s interval for the three additives in the data acquisition system (Table 23.2). The stabilization in temperature and pressure was considered as an indication of saturation of hydrate formation.



**Fig. 23.2** A schematic diagram of the setup used for natural gas hydrate formation experiments, where, SNG is synthetic natural gas cylinder; R1, R2 and R3 are reactors; P is pressure transducer; T is thermocouple; CU is cooling unit and DAQ is data acquisition system

**Table 23.2** Structural and experimental details of additives

Additives	Chemical structure	Molecular weight (g/mol)t	Molarity (M)	Volume of water (ml)	Number of moles
Oxalic acid		90.03	0.01	50	0.005
			0.05	50	0.025
Malonic acid		104.06	0.01	50	0.005
			0.05	50	0.025
Succinic acid		118.09	0.01	50	0.005
			0.05	50	0.025

### 23.2.3 Determination of Gas Consumption

The amount of gas present in the liquid phase at any time “t” is calculated by finding the difference between initial number of moles present in the gaseous phase and number of moles present in the gaseous phase at time “t”. The following formula can be used to find the same [15].

$$(\Delta n_{h,\downarrow})_t = \left( \frac{V_r P}{zRT} \right)_{t=0} - \left( \frac{V_r P}{zRT} \right)_{t=t} \quad (23.1)$$

where

$V_r$  = Volume of gaseous phase in the reactor,

$P$  = Pressure in the reactor,

$T$  = Temperature in the reactor,  $R$  = Universal gas constant and

$z$  = compressibility factor which is calculated using Pitzer’s correlation [16].

The rate of hydrate formation was calculated by forward difference formula as reported by Bhattacharjee et al. [15]:

$$\left( \frac{d(\Delta n_{h,\downarrow})_t}{dt} \right) = \frac{(\Delta n_{h,\downarrow})_{t=0} - (\Delta n_{h,\downarrow})_{t=t}}{\Delta t}; \text{ for every } t = 5 \text{ sec} \quad (23.2)$$

### 23.3 Results and Discussion

The typical gas hydrate formation kinetics curve is shown in Fig. 23.3 being obtained with the pure water system in the experimental setup, as described in Fig. 23.2. In the absence of the guest molecules (*mostly gaseous in nature*), water molecules exist in the form of pentamers and hexamers. These pentamers and hexamers rings are transient and highly labile due to molecular dynamics. During the course of gas hydrate experiments, in dissolution phase gas molecules enter water system which form labile clusters around dissolved gas molecules. The size of labile cluster depends on the number of surrounding water molecules, which ultimately depends on the size of the dissolved gas molecules. These labile clusters when combined together can form unit cells which upon reaching an ideal coordination number form hydrate.

This phenomenon is known as nucleation and essentially occurs at microscopic scale, hence nucleation point or induction time is taken as the time elapsed, until the appearance of detectable volume of hydrate phase or, equally, until the intake of detectable number of moles of hydrate former gas. It can be observed from the pressure profiles of the gas hydrates in the form of a sudden base shift, which may appear immediately or after a certain time interval depending upon the temperature/pressure gradients and the nature of the additive(s).

Here, in Fig. 23.3, which represents the data acquired before and after starting the shaker, a slight decrease in the pressure is observed, followed by sudden sharp decrease nearly at 200 s. The initial pressure drop is attributed to dissolution of gas in the liquid phase basically in the intermolecular spaces of the water molecules. A

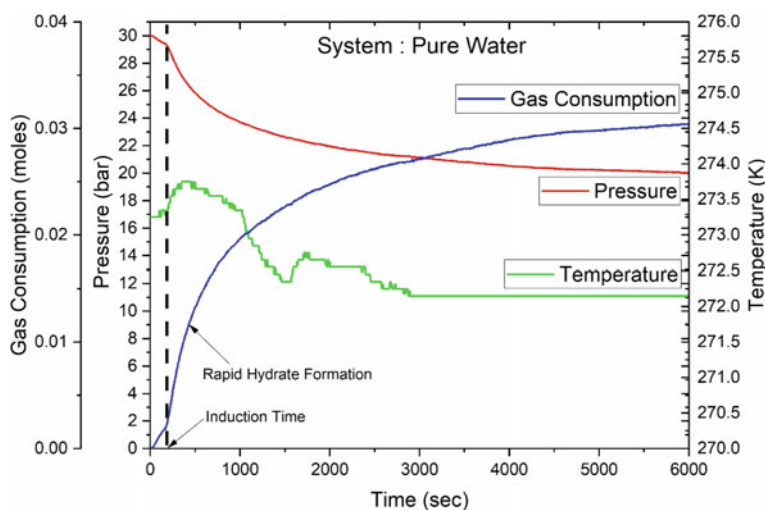


**Fig. 23.3** Pressure, temperature and gas consumption versus time for hydrate formation from pure water and synthetic natural gas system

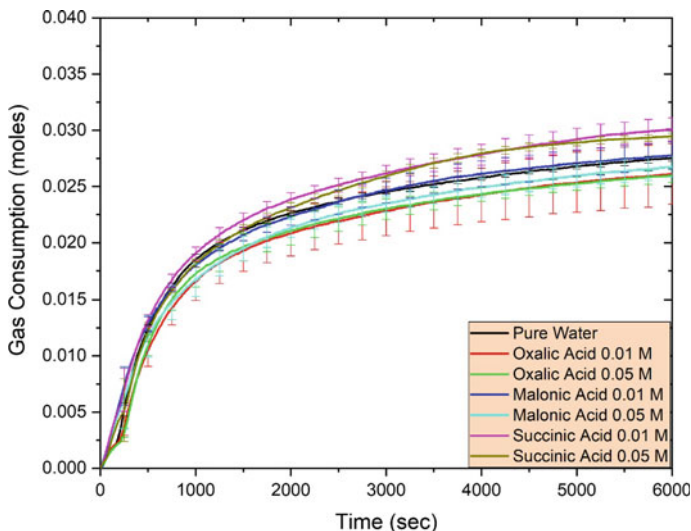


**Fig. 23.4** Comparison of gas hydrate formation kinetics of different additive systems represented by gas uptake behavior at different concentrations

sharp decrease in the pressure occurs due to formation of gas hydrate caged structures. As hydrate formation proceeds, gas molecules start moving from gas phase to liquid phase more rapidly. Induction time can be defined as a time at which first hydrate crystal is formed, after which quick hydrate formation takes place. We have considered induction time as the time at which a sudden pressure drop is observed along with the corresponding increase in the temperature. The sudden rise in the temperature at the induction point is due to the exothermic nature of hydrate formation or crystallization [2]. It should be noted that gas hydrate formation is equivalent to the formation of crystals, which is essentially an exothermic phenomenon and requires the consumption of heat by the surroundings for accelerated growth of the crystals.

Figure 23.4 shows the gas hydrate formation kinetics curves which are provided with error bars for all the systems under study. All the experiments were repeated for six times and their average plots are provided with the standard error bars. It is clear that oxalic acid at both concentrations (0.01 and 0.05 M) is having maximum inhibition characteristics as compared to the other two additive systems. Succinic acid at both the concentrations (0.01 and 0.05 M) displayed promoting characteristic when compared with pure water system, whereas malonic acid at 0.01 M showed mild inhibition behavior but at 0.05 M kinetics were similar to pure water system. Apart from the comparative gas uptake behavior, one more important observable trend corresponds to the concentration of the respective acids. It is evident that at higher concentrations the gas uptake kinetics slightly reduces than that of the same at lower concentrations. This trend is strictly followed in all of the three-acid molecule systems. The higher concentration gas uptake profiles lie below the low concentration gas consumption curves. The overall gas consumption pattern



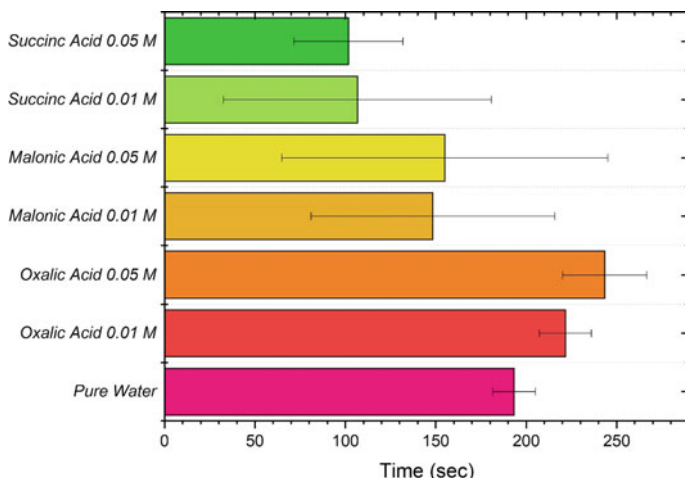


**Fig. 23.5** Induction time analysis (in seconds) for different additive systems under similar conditions of temperature and pressure. High induction time is indicative of the inhibition and low induction values indicate promotion behavior of the molecules

among the used additives was found to be oxalic acid < malonic acid < succinic acid. This sequence is in agreement with the regular increase in the number of nonpolar methylene units in the molecular backbone structures.

Figure 23.5 shows the comparison of induction time of additives, and an error bar is provided for this study. An increased induction time has been observed in case of the oxalic acid system when compared to water, which is an indicative of delayed nucleation [17]. As the concentration of oxalic acid was increased from 0.01 to 0.05 M, a further increase in induction time is observed. For the other two systems having additional methylene units such as malonic acid and succinic acid showed a decreased induction time at both the concentrations, when compared to the oxalic acid systems.

However, on increasing the concentration from 0.01 to 0.05 M an increase in the induction time is observed in all cases except succinic acid. Succinic acid in 0.05 M concentration showed least induction time in comparison with other systems. The decrease in the induction time and increased kinetics is a characteristic of promoting performance of any additive in gas hydrate studies and similar is the case here with the molecules having additional methylene units. Therefore, the behavior of all the systems can be explained on the basis of additive structures and functional moieties [18, 19].

From mechanistic point of view, the present additive systems provide deep structural insights into the factors responsible for hydrate growth or inhibition. Oxalic acid, malonic acid and succinic acid have carboxylic groups at the ends which are hydrophilic in nature, and thus enhance the solubility of the acids in the water. Carboxylic group consists of carbonyl group ( $-C=O$ ) and alcohol group ( $-O-H$ ), and the oxygen atom present in carbonyl group is highly electronegative which attracts

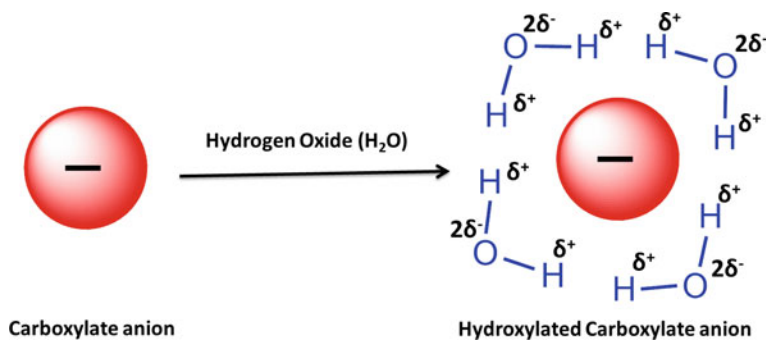


**Fig. 23.6** Schematic representation of hydration of carboxylic groups present in dicarboxylic acids. Carboxylate anions (-ve charged oxygen atom) attract water molecules by pulling hydrogen atoms (partially +ve charged) of water molecules

the electron pair in the alcohol group, which results in small positive charge on hydrogen atom and negative charge on oxygen atom (Fig. 23.6). The presence of carbonyl group ( $\text{-C}=\text{O}$ ) and hydroxyl group ( $\text{-O-H}$ ) in the gas hydrate system can be characterized by using FT-IR spectroscopy either in ATR or normal modes. In FTIR, the carbonyl group peak usually ranges from  $1700$  to  $1780\text{ cm}^{-1}$  and hydroxyl group peak ranges from  $3100$  to  $3600\text{ cm}^{-1}$  with some variations due to space interactions with other functional groups and electronic interactions (which can be studied by UV spectroscopy) [20–22].

The induced charges result in enhanced polarity in water molecules, which increases the hydrogen bonding with neighboring water molecules. This is exactly required for the formation of hydrogen bonds and an essential requisite for the same in order to form cage-like structures [17]. When oxalic acid enters the water, both the carboxylic groups engage free water molecules with hydrogen bonding interactions. Thus, leaving less water molecules available for hydrate formation which results in delay in nucleation as well as reduced kinetics because of unavailability of sufficient free water molecules [23]. This is the case with the oxalic acid system that represents the least kinetics among the three-acid systems.

As the chain length increases in the di-acid molecules, the number of  $\text{-CH}_2$  units present between two carboxylic ends also increases. Since,  $\text{-CH}_2$  units are hydrophobic in nature, there is an increase in the solubility of nonpolar gas molecules with increase in the chain length of di-acids in the di-acid water solutions. Also, the presence of  $\text{-CH}_2$  units pull out or disturb the attraction between the acid and water molecules, thus negatively affect the interaction between carboxylic groups and water molecules. These hydrophobic units can also act as small pouches for hydrophobic gas molecules which enter water system during the pressurization [17]. Usually, guest molecules under the gas hydrate study systems coordinate with the water molecules via Van der Waals forces to form cage-like structures. These hydrophobic pockets can act as habitation sites for methane, ethane, n-butane and isobutane present in the SNG, thus increasing the dissolution of gas molecules in the water, thereby favoring

the gas hydrate formation by increasing their relative availability. Therefore, these factors are most possible explanation for gradual variation from comparatively inhibition behavior of oxalic acid to observe promotion behavior of succinic acid when considering the three acids in the present work.

## 23.4 Conclusion

Three additives, namely oxalic acid, malonic acid and succinic acid, with low molecular weight and high solubility in the water were investigated at two concentrations of 0.01 and 0.05 M for inhibition/promotion activity in gas hydrate formation at 273.15 K and 3.0 MPa in shaker bed apparatus. The gas hydrate formation kinetics and induction time data were analyzed. The hydrate former gas consumption pattern was found to be in the following order: oxalic acid < malonic acid < succinic acid. On the basis of gas formation kinetics and induction time data, we report oxalic acid as probable natural gas hydrate inhibitor. Because of small molecular weight and biodegradability, oxalic acid becomes an attractive option as a KHI. However, to get optimal concentration of oxalic acid for adequate performance, there is a requirement of more fundamental detailed studies using spectroscopic and calorimetric tools such as XRD, Raman and DSC.

**Acknowledgments** Dr. Kushwaha acknowledges Department of Science and Technology, Science and Engineering Research Board, India for the project grant DST-SERB-PDF-2017/003075 as a principal investigator at IIT-Madras, and Council of Scientific and Industrial Research, India for CSIR-RA-31/11(954)/2017-EMRI at CSIR-NCL, Pune.

## References

1. T.S. Collett, V.A. Kuuskraa, *Oil Gas J.* **96**, 90–95 (1998)
2. E.D. Sloan, *Nature* **426**(6964), 353–363 (2003)
3. A. Kumar, T. Sakpal, P. Linga, R. Kumar, *Chem. Eng. Sci.* **122**, 78–85 (2015)
4. M. Tariq, D. Rooney, E. Othman, S. Aparicio, M. Atilhan, M. Khraisheh, *Ind. Eng. Chem. Res.* **53**, 17855–17868 (2014)
5. M.A. Kelland, *Energy Fuels* **20**, 825–847 (2006)
6. T.A. Strobel, K. Hester, C. Koh, A. Sum, E.D. Sloan Jr., *Chem. Phys. Lett.* **478**, 97–109 (2009)
7. J.A. Ripmeester, J.S. Tse, C.I. Ratcliffe, B.M. Powell, *Nature* **325**, 135–136 (1987)
8. E.D. Sloan, *Ind. Eng. Chem. Res.* **39**, 3123–3129 (2000)
9. I. Chatti, A. Delahaye, L. Fournaison, J.-P. Petit, *Energy Convers. Manag.* **46**, 1333–1343 (2005)
10. S.K. Kelkar, M.S. Selim, E.D. Sloan, *Fluid Phase Equilib.* **150–151**, 371–382 (1998)
11. R.L. Reed, L.R. Kelley, D.L. Neumann, R.H. Oelfke, W.D. Young, *Ann. N. Y. Acad. Sci.* **715**, 430–446 (1994)
12. M.A. Kelland, T.M. Svartaas, L. Dybvik, *Offshore Europe*, Society of Petroleum Engineers, pp. 531–539 (1995)

13. C.A. Koh, R.E. Westacott, W. Zhang, K. Hirachand, J.L. Creek, A.K. Soper, *Fluid Phase Equilib.* **194–197**, 143–151 (2002)
14. S. Alavi, S. Takeya, R. Ohmura, T.K. Woo, J.A. Ripmeester, *J. Chem. Phys.* **133**, 074505 (2010)
15. G. Bhattacharjee, A. Kumar, T. Sakpal, R. Kumar, *A.C.S. Sustain. Chem. Eng.* **3**, 1205–1214 (2015)
16. J.M. Smith, H.C. Van Ness, M. Abbott, *Introduction to chemical engineering thermodynamics*, Chapter 3, pp. 99–109 McGraw-Hill (2010)
17. S.B. Meshram, O.S. Kushwaha, P.R. Reddy, G. Bhattacharjee, R. Kumar, *Chinese J (Chem, Eng, 2019)*. in press
18. G. Bhattacharjee, V. Barmecha, O.S. Kushwaha, R. Kumar, *J. Chem. Thermodyn.* **117**, 248–255 (2018)
19. G. Bhattacharjee, O.S. Kushwaha, A. Kumar, M.Y. Khan, J.N. Patel, R. Kumar, *Ind. Eng. Chem. Res.* **56**, 3687–3698 (2017)
20. O.S. Kushwaha, C.V. Avadhani, R.P. Singh, *Carbohydr. Polym.* **123**, 164–173 (2015)
21. O.S. Kushwaha, C.V. Avadhani, R.P. Singh, *Adv. Mater. Lett.* **5(5)**, 272–279 (2014)
22. S. Aiyer, R. Prasad, M. Kumar, K. Nirvikar, B. Jain, O.S. Kushwaha, *Appl. Mater. Today* **4**, 71–77 (2016)
23. G. Bhattacharjee, N. Choudhary, V. Barmecha, O.S. Kushwaha, N.K. Pande, P. Chugh, S. Roy, R. Kumar, *Appl. Energy* **253**, 113566 (2019)